HEAT FLOW OVER THE EQUATORIAL MID-ATLANTIC RIDGE

by

Robert Allin Folinsbee

B.Sc., University of Alberta

(1964)

SUBMITTED IN PARTIAL FULFILLMENT

OF THE REQUIREMENTS FOR THE

DEGREE OF MASTER OF

SCIENCE

at the

MASSACHUSETTS INSTITUTE OF

TECHNOLOGY

January, 1969

Signature of Author_____

Department of Geology and Geophysics
January 23, 1969

Certified by_____

Thesis Supervisor

Accepted by_____

Chairman, Departmental Committee
on Graduate Students

HEAT FLOW OVER THE EQUATORIAL MID ATLANTIC RIDGE

Robert Allin Folinsbee

Submitted to the Department of Geology and Geophysics on January 23, 1969 in partial fulfillment of the requirement for the degree of Master of Science.

Forty-six heat flow measurements were made over the Equatorial mid-Atlantic ridge and the Vema fracture zone. The heat flow near the median valley of the ridge is high and varies from 1.7 - 11 HFU. The very high values appear to be caused by near surface tectonic activity occuring along parts of the median valley. The heat flow decreases to 1 HFU 100 km from the axis, and increases to more than 2 HFU 200 km from the axis. These alternating zones of high and low heat flow may be associated with the pause in sea floor spreading that ended about 10 million years ago. The heat flow in the northern valley of the Vema fracture zone averages 3.1 HFU with a standard deviation of only 0.18 HFU. The high uniform heat flow is due to tectonic processes occurring along this active portion of the fracture zone. The heat flow in the remainder of the fracture zone appears similar to that seen on the ridge immediately to the north of the fracture zone, indicating that the southern portion of the fracture zone is presently not an active fracture zone.

Thesis Supervisor: M. Gene Simmons
Title: Professor of Geophysics

TABLE OF CONTENTS

Abstract 2

Table of Contents 3

Introduction 4

Instrumentation and Data Reduction 6

Results 10

Interpretation 12

Summary 17

Bibliography 19

Figures: 21ff

- Fig. 1 Map showing the area of study
- Fig. 2 Temperature depth profile at station CH 75-31
- Fig. 3 Heat flow profile along 11°30'N
- Fig. 4 Heat flow profile along 13°30'N
- Fig. 5 Heat flow profile along 13°30'N out to 1500 km from the ridge axis
- Fig. 6 Map showing heat flow over the Vema fracture zone and over the crestal region of the ridge
- Fig. 7 Heat flow profile across the northern valley of the Vema fracture zone
- Fig. 8 Heat flow profile over the southern part of the Vema fracture zone
- Fig. 9 Composite heat flow profile
- Fig. 10 Effect on the heat flow of differing time intervals since the resumtion of sea floor spreading
- Fig. 11 Average heat flow over the mid-Atlantic ridge system

Table 1 Summary of heat flow data 32

Appendix A Compilation of all available data for each heat flow station 34

INTRODUCTION

Forty-six heat flow measurements were made near the Equatorial mid-Atlantic ridge. The first set of measurements was made in the vicinity of the Vema fracture zone, and the second set was made between the Lesser Antilles and the mid-Atlantic ridge. Bathymetric and magnetic profiles were obtained in both areas, and gravity and reflection seismic profiles were obtained between the ridge and the Lesser Antilles. The location of the area studied is shown in fig. 1.

Previous work done in the area includes that of Ewing et al. (1966) on the sediment distribution in the Equatorial and South Atlantic. Langseth et al. (1966) compiled the heat flow values in the Atlantic, fitted a polynomial surface to them and made deductions about the continuity of sea floor spreading in the Atlantic. They found that the lack of a broad heat flow anomaly over the mid-Atlantic ridge indicated that sea floor spreading had stopped at least 10 m.y. ago, and had resumed again only recently. McKenzie et al. (1967) were able to fit the observed heat flow profile without requiring an interruption in sea floor spreading by using a different model.

Van Andel and Bowin (1968) made a detailed study of the ridge at 20 °N (about 700 km north of the area where the new heat flow measurements were made). They found the

ridge was divided into several physiographic zones running parallel to the ridge axis. The floor of the median valley consists of fresh basalts, while the walls consist of low grade metamorphic rocks and older basalts. A crestal region extends out to 100 km from the ridge axis and is marked by a lack of sediment. At the boundary between the crestal region and the upper flank region the sediment depth increases rapidly to as much as 250 m, indicating that the upper flank region is of Miocene age, while the crestal region is no older than Quaternary. Magnetic evidence indicates that the spreading rate of the crestal region is about 1.4 cm/yr. There appears to be a period of quiescence between the formation of the upper flank region and the formation of the crestal region.

Phillips (1967) obtained magnetic profiles across the ridge at 20 °N and 27 °N. Theoretical profiles calculated assuming a spreading rate of 1.4 cm/yr agreed with the observed profiles out to 80 km from the axis. Beyond 80 km it was necessary to assume a spreading rate of 1.7 cm/yr to obtain agreement, indicating a discontinuity in the spreading rate at about 6 million years ago.

The Vema fracture zone offsets the mid-Atlantic ridge at 11 °N. The topography of this region has been studied by van Andel et al. (1967). The Vema fracture zone consists of at least 3 valleys running east-west. The floor of the

northern valley is 2 km below the level of the ridge flanks, and the valley has been filled with more than 1 km of flat lying sediment. The south wall of the valley is 2.5 km high with side slopes of 30-45°. To the south there are 2 or more subsidiary valleys which appear to be presently inactive. Sykes (1967) has calculated the epicentral location and direction of first movement of earthquakes occurring near the mid-Atlantic ridge. There were 7 earthquakes in the Vema fracture zone, all located in the northern valley or on the valley walls. The direction of first motion (available for only one earthquake) indicates that transform faulting is occurring along the Vema fracture zone.

INSTRUMENTATION AND DATA REDUCTION

The heat flow measurements for this study were made with two types of instruments. When a piston core was taken, a Ewing thermograd recorder (Langseth, 1965) with outrigger thermistors mounted on the barrel was used. In regions where little sediment was expected or no core was desired, a Scripps short probe (Von Herzen et al., 1962), a 2 m stainless steel tube with internal thermistors, was used. Temperatures were measured with the piston corer over distances up to 12 m, and with the short probe over distances up to 2 m. For the piston core apparatus the water temperature was recorded (at the top of the weight stand), as was the difference in temperature

between the water and the individual probes on the barrel. The errors in temperature due to errors in calibration and in reading the records are small, about 0.002 °C. Larger errors (up to 0.010 °C) were caused by the probes not reaching a steady temperature while they were in the bottom. This occurred only occasionally and may have been due to movement of the corer after penetration. The distance between the individual probes was measured before and after the core was taken to eliminate errors caused by movement of the probes on the barrel. The accuracy of the measurement was better than 1 cm.

The thermal conductivities were measured every 50 cm on the piston cores using the needle-probe technique described by Von Herzen and Maxwell (1959). The measurements were repeatable to within 2%, but errors in calibration of the needle and in the determination of the average conductivity of the core raise the error in the conductivity measurements to 4-5%. At the short probe stations no core was obtained; therefore it was necessary to assume a conductivity for these stations based on the conductivity of nearby piston cores. Since the piston core conductivities vary between 2.12-2.55 x 10^{-3}cal/ °C cm sec, while the assumed conductivities are about 2.3 x 10^{-3}cal/ °C cm sec, the additional error introduced by this procedure is probably less than 10%.

For stations where there was no regular change in the conductivity with depth, an average thermal gradient was obtained

from the temperature depth data by a least squares procedure. An estimated error in the gradient was calculated from the uncertainties associated with the individual temperature measurements and from the difference between the observed temperature and that predicted by the least squares fit.

When the conductivity varied regularly along a core the thermal gradient between successive probes was multiplied by the average conductivity between the probes to obtain a value for the heat flow. A weighted average of these values was then used to calculate the heat flow at the station.

At station VFZ-13 the water temperature is 0.014 °C greater than the temperature of the sediment at probe 1. The measured heat flow between successive probes is 0.38, 0.21 and 1.16 HFU[1]. The reduction of the sediment temperature does not appear to have been caused by the deposition of material carried from a more shallow depth, as in this case the temperature of the newly deposited sediment would be higher than that of the water. The change appears to be due to an increase in the temperature of the bottom water. A single increase in the bottom temperature results in a measured heat flow that increases with depth and a deviation from the true heat flow that decreases with depth. The heat flow observed at this station may be the result of several increases and decreases in water temperature, with the latest change being an increase.

---

[1] HFU = heat flow units $\mu cal/cm^2 sec$

At station CH-75-31 the gradient is reversed (-0.007 ^{o}C/m) between probes 2 and 3, and is low (0.005 ^{o}C/m) between probes 4 and 5. Between probes 1 and 2, and between 3 and 4, the gradient is higher (0.026 and 0.036 ^{o}C/m). This may be caused by the effect of a periodic change in the water temperature superimposed on a linear gradient. In fig. 2 we can see that the apparent wavelength of the temperature disturbance in the sediment is about 3.5 meters.

Carslaw and Jaeger (1959) derive the formula for the temperature in a halfspace due to a sinusoidal oscillation ($T_o \cos(\omega t)$) at the surface. The temperature is given by

$$T = T_o \exp(-kz)\cos(\omega t - kz)$$

z = distance from surface

$k = (\omega/2K)^{1/2}$

K = diffusivity

and the wavelength λ is

$$\lambda = (4\pi KP)^{1/2}$$

where P is the period ($2\pi/\omega$).

If the wavelength is taken to be 3.4 meters, and the diffusivity to be 0.005 cm^2/sec, the period of the temperature disturbance is about 27 days. The amplitude of the change of the bottom water temperature necessary to cause the

deviation is about 1 °C.

At station CH 75-14 the gradient between probes 2 and 3 is reversed (-0.007 °C/m), and the gradient between probes 1 and 2 is positive (0.028 °C/m). The other probes did not record at this station. Therefore the wavelengt of the disturbance cannot be calculated at this station, but the gradient is similar to that seen at CH 75-31. The average heat flow at both these stations is small, which makes small disturbances in the thermal gradient more apparent.

RESULTS

A complete listing of the data obtained at eacn station is given in appendix A. The heat flow, position, water depth, thermal gradient, and average conductivity at each station are summarized in table 1. For the consideration of the results the heat flow stations are grouped into 3 sets: 16 stations in the Vema fracture zone, 12 stations on the ridge at 11°30'N , and 18 stations on the ridge at 13°30'N.

In fig. 3 a profile of the heat flow just to the north of the Vema fracture zone (11°30'N) and extending out to 250 km on both sides of the ridge is given. The measurement closest to the ridge axis (30 km distance) shows a heat flow of 2.4 HFU. To the west of the axis the heat flow decreases to 0.8 HFU 100 km from the axis, increases to 2.3 HFU 200 km from the axis, and then decreases again. On the east side of

the ridge the first measurement is 100 km from the axis and shows a heat flow of 0.5 HFU. The heat flow increases to 2.3 HFU 190 km from the axis, and then decreases to about 1 HFU.

At 13°30' there were fewer measurements within the crestal region of the ridge. To the east of the ridge there are only 2 measurements, 1.6 HFU 70 km from the axis, and 0.5 HFU 180 km from the axis. One measurement made in the median valley showed a temperature gradient so large that the recorder went off scale. Calculations showed that for this to happen the heat flow must have been greater than 11 HFU. A profile of the heat flow to the west of the median valley in the crestal region is shown in fig. 4. The heat flow decreases from greater than 4.2 HFU near the median valley to 1.9 HFU 100 km from the axis. At 175 km the heat flow is 2.5 HFU and at 270 km the heat flow has decreased to 1.2 HFU.

Figure 5 shows the heat flow at 13°30'N out to 1500 km from the axis. Between 300 and 600 km distance there is a region of low heat flow (average = 0.9 HFU). In the basin region, which begins 800 km from the axis, the heat flow is quite uniform with an average of 1.28 HFU and a standard deviation of 0.23 HFU. At 58 °W the heat flow is lower, with the average of 3 values near there being 1.0 HFU.

The heat flow is high for the stations in the Vema

fracture zone with an average value of 2.1 HFU, although values as low as 0.5 HFU are also found. The measurements in this region, along with those near the ridge to the north, are shown in fig. 6. The heat flow on the floor of the main valley is high (3.0 HFU) and very uniform (standard deviation 0.18 HFU). Three of the measurements that are in a closely spaced north-south profile across the floor of the valley are shown in fig. 7.

The remaining heat flow measurements lie in that part of the Vema fracture zone believed to be inactive. These values are plotted against the distance from the axis of the southward continuation of the ridge. Values between 1.1-4.3 HFU were found near the median valley. A value of 0.3 HFU was recorded 100 km from the axis, while 200 km from the axis values of 2.3 and 5.1 HFU were recorded. Further to the west the heat flow decreases to values of 1.0, 0.9, and 0.5 HFU.

INTERPRETATION

The pattern of heat flow over the mid-Atlantic ridge between 10-14 °N shows some similarities to that seen over other parts of the ridge. There is a narrow axial zone of high, but widely varying, heat flow. The anomaly is most evident in the northern profile, where values of 4.2 and 11 HFU are found near the median valley. The value of 11 HFU is one of the highest measured along the mid-Atlantic

ridge, and it indicates that there has been recent tectonic activity in the area. Another indication of recent tectonic activity in the axial zone is the fresh basalt dredged from the median valley by van Andel and Bowin (1968). To the south the heat flow near the axis (within 50 km) varies between 1.1 and 4.3 HFU and the average value is 2.4 HFU. The variability indicates that the tectonic activity has not occurred continuously along the axis.

The heat flow decreases rapidly with increasing distance from the axis, as can be seen in fig. 9. This profile includes all the heat flow measurements made in the area with the exception of the 6 measurements made in the northern valley of the Vema fracture zone. The 6 measurements are excluded since the northern valley is presently active, and the heat flow there does not appear to be related to the distance from the ridge. The measurements from the southern part of the Vema fracture zone appear to be unaffected by the fracture zone, since the heat flow profile in this region has the same shape as the profile to the north of the Vema fracture zone.

At a distance of 100 km from the axis, which corresponds to the boundary between the crestal and upper flank region, the average heat flow is less than 1 HFU. Throughout the period for which sea floor spreading had ceased, the material now at the boundary between the crest and the upper flank was located over the ridge axis. During this period cooling of

the material may have occurred not only by thermal conduction, but also through volcanic activity along the axial region of the ridge. This additional cooling would result in very low values of heat flow near the boundary between the crestal and upper flank regions.

In the region outside the crest-flank boundary the heat flow should increase since there would have been no volcanic activity over this region during the quiescent period. Between 160 km and 250 km from the ridge there are 5 values of heat flow greater than 2 HFU and only 1 reliable value of less than 2 HFU. However, beyond 260 km the heat flow is normal and the narrowness of this zone of high heat flow is heard to explain. Using the results from Langseth et al. (1966) the shape of the expected heat flow anomaly outside the ridge-flank boundary can be determined. The profiles in fig.10 show the heat flow for differing periods of quiescence. The theoretical heat flow decreases very gradually with increasing distance from the ridge, unlike the observed heat flow. This indicates that much of the high heat flow must be due to some other source. A possible explanation is that the change that occurred in the convection cell and caused the cessation of sea floor spreading may also have altered the structure or composition of the crustal material being formed prior to the cessation. The crust may have been enriched in heat producing minerals or the mantle material beneath this area of the ridge may be at an above normal

temperature.

This bimodal pattern has been observed on other profiles made across oceanic ridges. Chessman et al. (1968) made a series of 9 measurements across the Reykjanes ridge. No measurements were made on the axis of the ridge, but the measurements on the sides showed high heat flow on both sides of the axis, with the heat flow decreasing as the axis was approached. The separation between the two peaks was 50 km. Von Herzen and Uyeda (1963) made a series of closely spaced measurements across the East Pacific rise. They found a zone of high heat flow along the crest of the rise and adjacent zones of high heat flow 150 km on either side of the rise. These two structures may be caused by the same mechanism producing this structure over the Equatorial mid-Atlantic ridge.

The low values of heat flow recorded on the flanks of the ridge are in agreement with the low heat flow found in this region by Lee and Uyeda (1965) which may be due to a systematic error that reduces the observed heat flow. Increases in the roughness of the bottom will reduce the observed heat flow, as well as increase the scatter in the measurements. Near the bottom the isothermal surfaces in the sediment conform to the shape of the topography, and thus the thermal gradient measured with a vertical arrangement of probes is less than the actual value. The actual thermal

gradient is also lower than would be measured on a flat surface; since the area of contact between the water and the sediment is increased, the heat flux per unit surface area is less. Taking the two effects into account yields the following relationship (from Lachenbruch and Marshall, 1966):

$$(q^* - q_v)/q^* \doteq \sin^2 \bar{\theta}$$

q^* = true regional heat flow

q_v = average vertical heat flow

$\bar{\theta}$ = average slope of the bottom

It requires average slopes of 20° to reduce the heat flow by 15%. The perturbation in the thermal gradient will penetrate the sediment to a depth approximately equal to wavelength of the topographic feature and since the gradients are measured over a maximum distance of 10 m, topography with a wavelength greater than 10 m will reduce the heat flow. The depth recorders used are incapable of resolving features smaller than 200 m across at the depths of the flank region. The large scale topography in the region has slopes of about 5°, and if small scale topography has average slopes of about 15° the reduction in heat flow appears to be about 20%, but there are only 2 reliable measurements in the region,

and the scatter introduced by the topography can easily account for this difference.

The heat flow is very uniform in the basin region to the west of the ridge. The average heat flow is 1.28 HFU, which is close to the mean value of 1.3 HFU for all the Atlantic basins reported by Lee and Uyeda (1965). The uniformity indicates that this region has been tectonically inactive for a long period of time and possesses a uniform crustal structure. The lower heat flow near 57 °W may be the result of the down going limb of a convection cell. The anomaly associated with the down going limb is narrow, with low heat flow occurring only within 50 km of the axis of the cell (Langseth et al., 1966).

SUMMARY

The measurements made over the Equatorial mid-Atlantic ridge show a high heat flow in the axial due to the rising convection cell located there. Very high heat flow in some parts of the median valley indicates that recent volcanic activity has occurred in this region. The heat flow decreases away from the ridge to below normal values (less than 1 HFU) at the crest-flank boundary, 100 km from the axis. The narrowness of the zone of high heat is a result of the pause in sea floor spreading that ended about 10 million years ago.

Beyond the crest flank boundary the heat flow increases to about 2.0 HFU on both sides of the ridge. The bimodal

structure may be due to a change in the composition of the crustal material formed prior to the cessation of sea floor spreading, or it may be due to an increase in the temperature of the mantle underlying this region. Beyond this region the heat flow on the flanks is low, probably due to the systematic reduction of the heat flow because of large topographic variation.

The heat flow in the basin to the west of the ridge is quite uniform, indicating that this region possesses a uniform crustal structure and has been tectonically inactive for a long period of time.

The high heat flow and earthquake activity occurring in the northern valley of the Vema fracture zone indicate that this is presently an active region. The heat flow in the remainder of the fracture zone is similar to that measured over the ridge to the north of the fracture zone, and does not appear to be affected by the fracture zone. Thus the southern part of the fracture zone is probably inactive.

ACKNOWLEDGMENT

This work was supported by the Office of Naval Research under contract Nonr 1841(74)

BIBLIOGRAPHY

Carslaw, H. S., and J. C. Jaeger, Conduction of Heat in Solids, 2nd edition, Clarendon Press, Oxford, 1959.

Chessman, M., K Horai, and G. Simmons, Heat flow over the Reykjanes ridge south of Iceland, Trans. American Geophys. Union, 49, 324, 1968.

Ewing, M., X. Le Pichon, and J. Ewing, Crustal structure of the mid-ocean ridges, 4, J. Geophys Res., 71, 1611, 1966.

Lachenbrauch, A., and B. Marshall, Heat flow through the Arctic ocean floor: the Canada Basin-Alpha rise boundary, J. Geophys. Res., 71, 1223, 1966.

Langseth, M., X. Le Pichon, and M. Ewing, Crustal structure of the mid-ocean ridges, 5, J. Geophys. Res., 71, 5321, 1966.

Lee, W., and S. Uyeda, Review of heat flow data, in Terrestrial Heat Flow, edited by W. Lee, Geophys. Monongraph 8, pp 87-190, American Geophysical Union, Washington, D. C., 1965.

Le Pichon, X., Sea floor spreading and continental drift, J. Geophys. Res., 73, 3661, 1968.

McKenzie, D., Some remarks on heat flow and gravity anomalies, J. Geophys. Res., 72, 6261, 1967.

Phillips, J., Magnetic anomalies over the mid-Atlantic ridge near 27°N latitude, Science, 157 (3791), 920, 1967.

Sykes, L., Mechanism of earthquakes and nature of faulting on the mid-ocean ridges, J. Geophys. Res., 72, 2131, 1967.

Vacquier, V., and R. Von Herzen, Evidence for connection between heat flow and the mid-Atlantic ridge magnetic anomaly, J. Geophys. Res., 69, 1093, 1964.

van Andel, T., and C. Bowin, Mid-Atlantic ridge between 22° and 23° north latitude and the tectonics of mid-ocean rises, J. Geophys. Res., 73, 1279, 1968.

van Andel, T., J. Corliss, and V. Bowen, The intersection between the mid-Atlantic ridge and the Vema fracture zone in the North Atlantic, J. Marine Res., 25, 343, 1967.

Veronis, G., and H. Stommel, The actions of varriable wind stresses on a stratified ocean, J. Marine Res., 15, 75, 1956.

Von Herzen, R., and A. Maxwell, The measurement of thermal conductivity of deep-sea sediments by a needle-probe method, J. Geophys. Res., 64, 1557, 1959.

Von Herzen, R., and S. Uyeda, Heat flow through the eastern Pacific Ocean floor, J. Geophys. Res., 68, 4219, 1963.

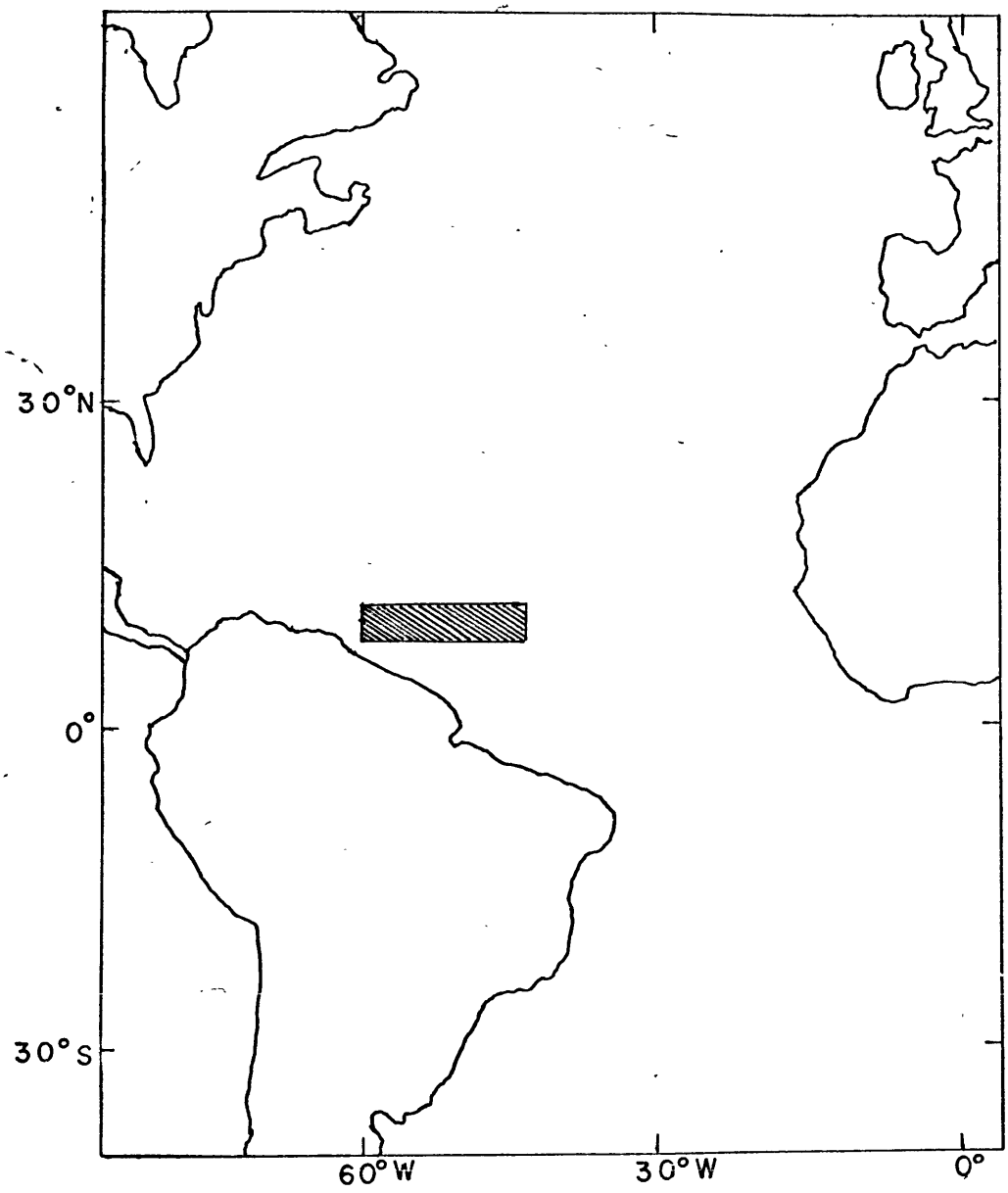

Fig. 1 Map showing area studied (shaded portion)

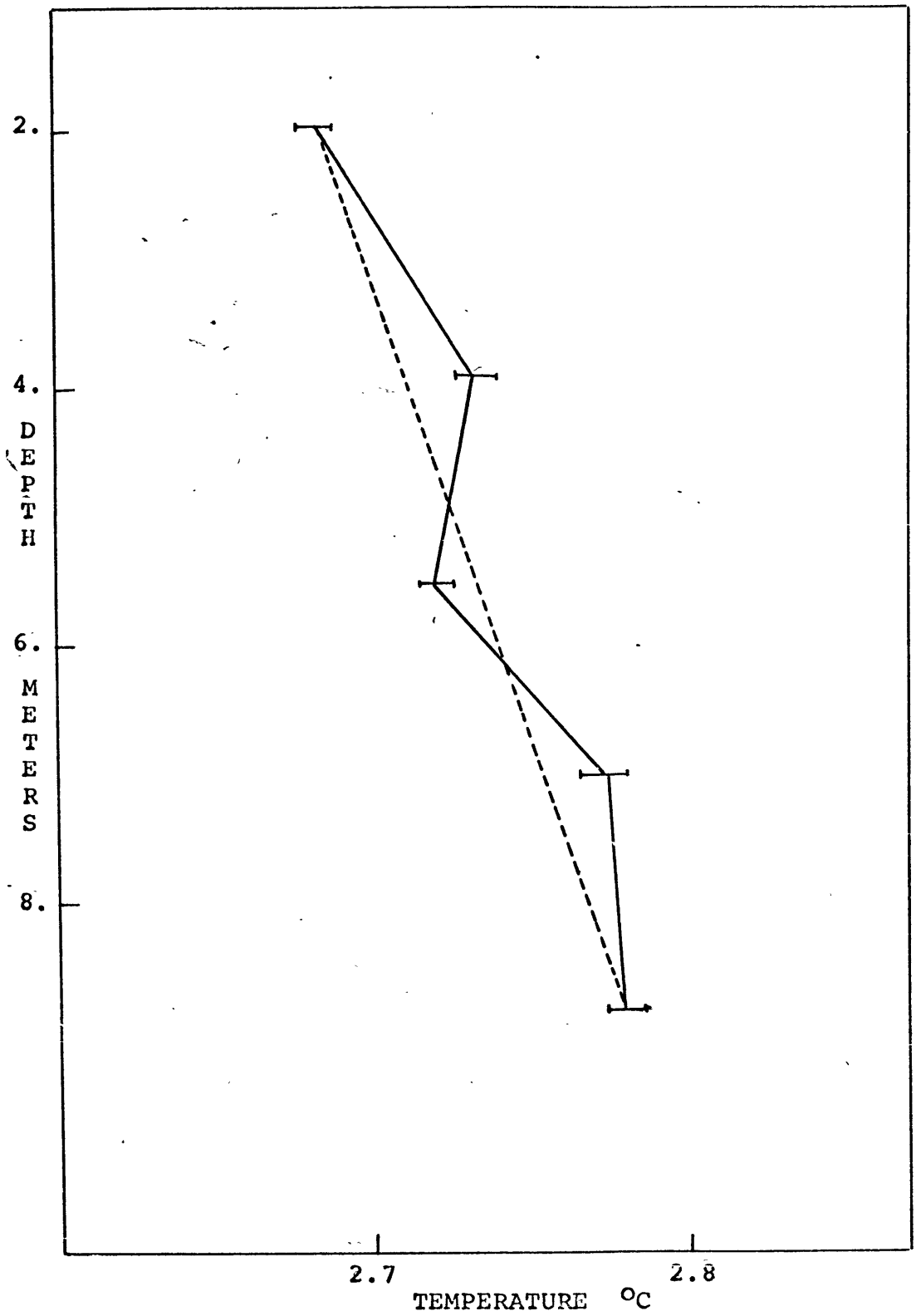

Fig. 2 Temperature-depth profile at station CH 75-31 showing the deviation of the observed temperature gradient from a linear temperature gradient. The horizontal bars indicate the error associated with the temperature measurement.

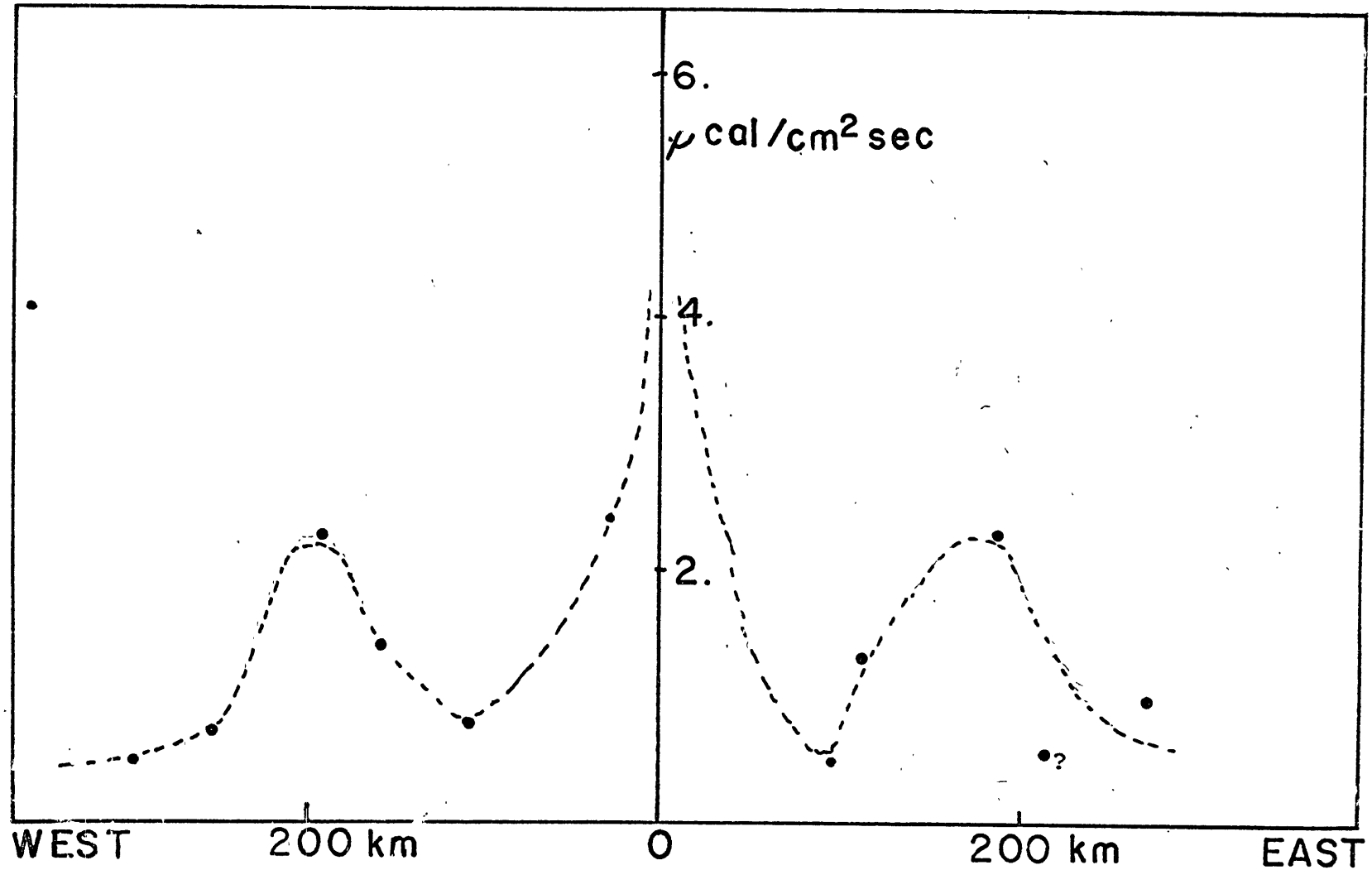

Fig. 3 Heat flow profile across the Mid-Atlantic Ridge at 11°30' N.

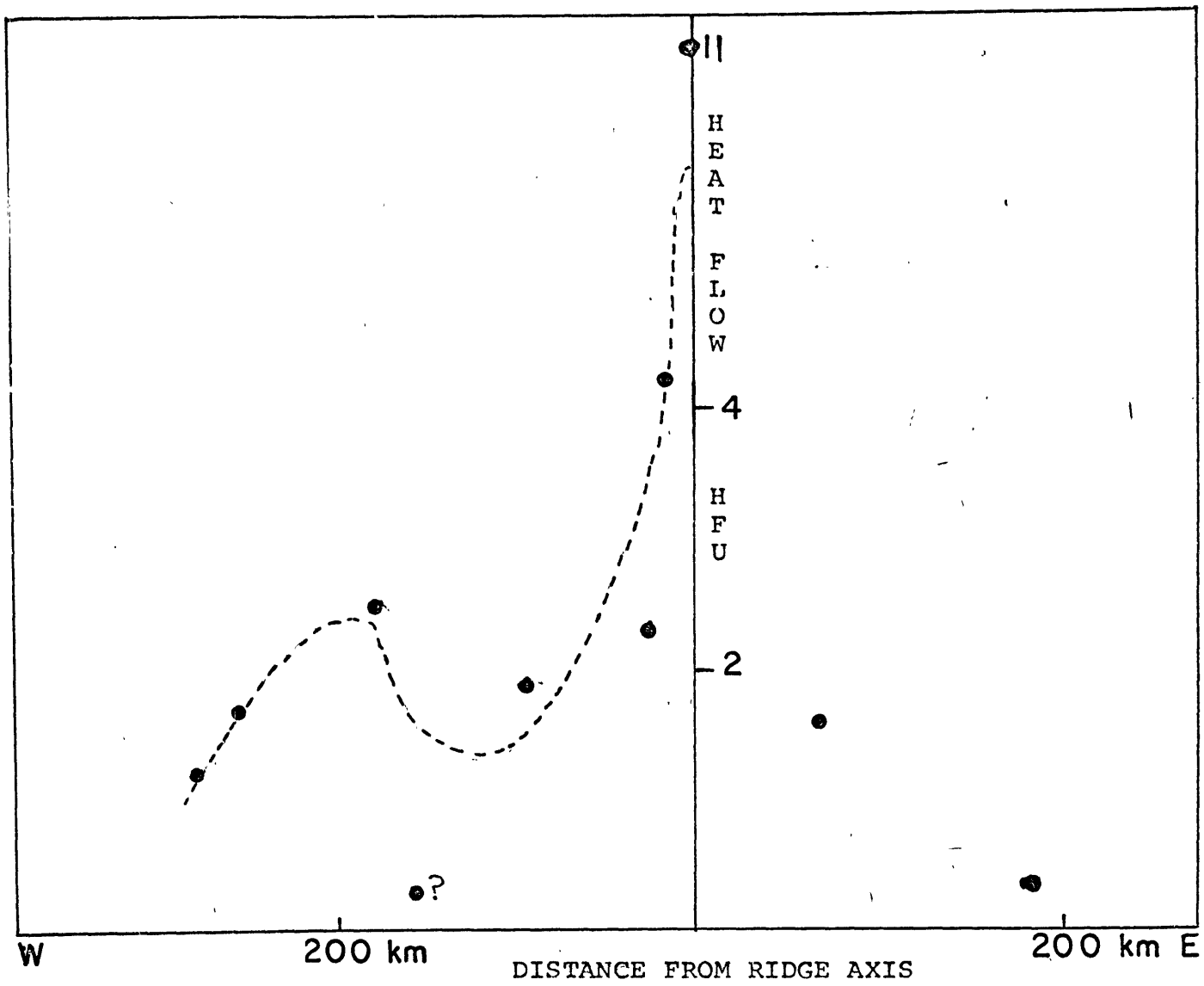

Fig. 4 Heat flow profile across the mid-Atlantic ridge at 13°30'N.

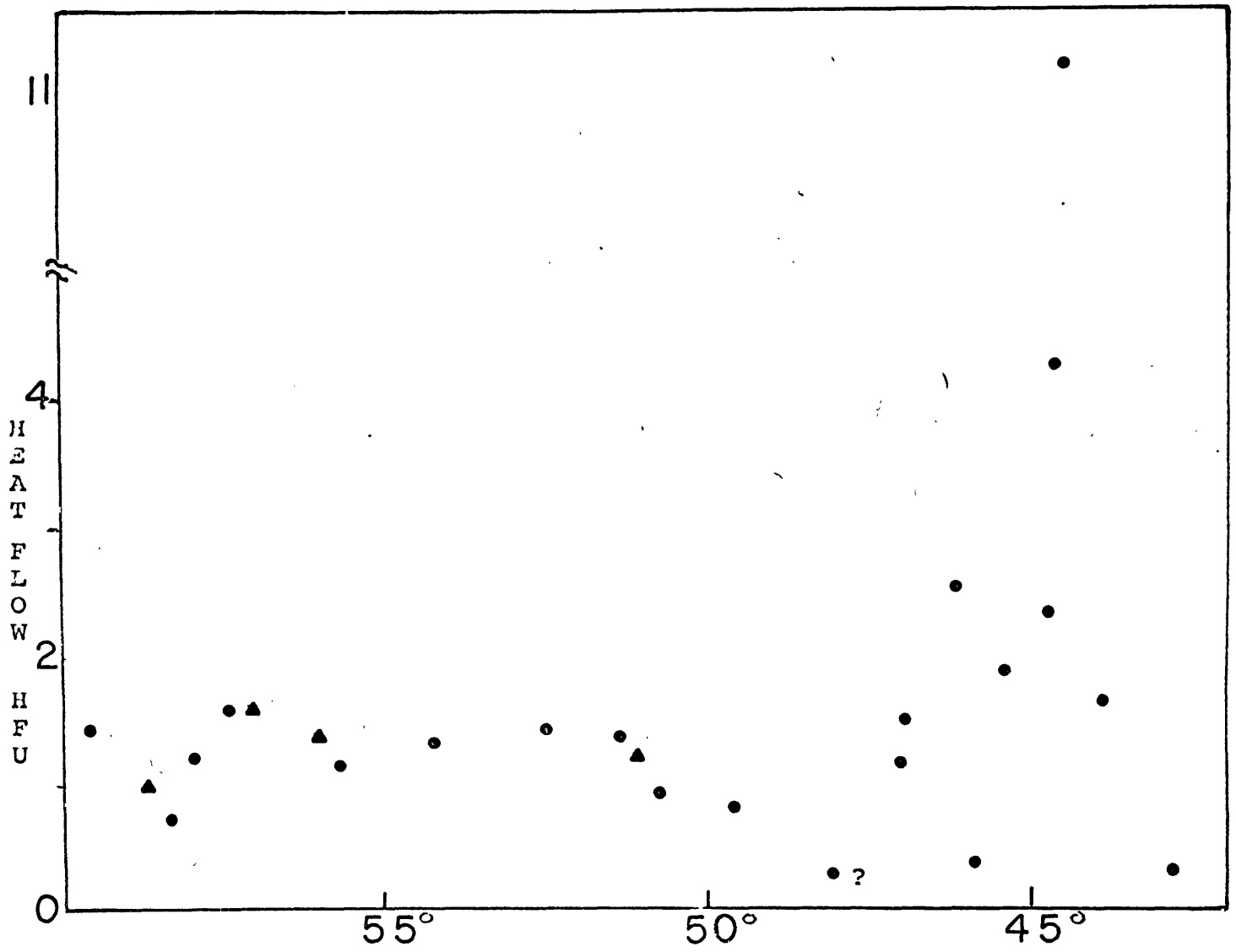

Fig. 5 Heat flow values at 13°30'N from the Lesser Antilles Arc to the Mid Atlantic Ridge plotted versus lattitude. Circles are new values triangles are previously published data. The ridge axis is at 44°30'N.

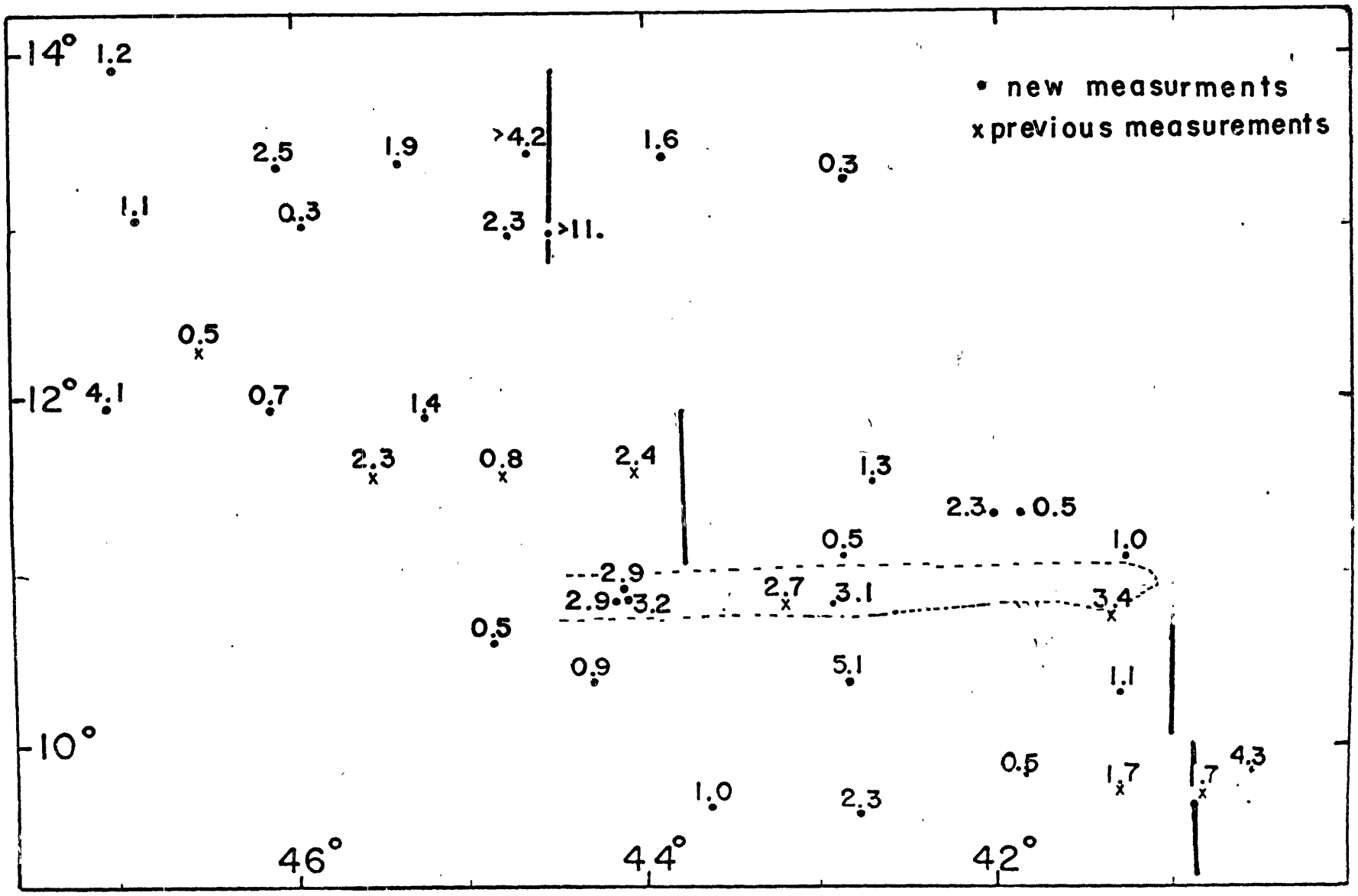

Fig. 6 Heat flow values near the Mid-Atlantic Ridge. Solid lines indicate the location of the median valley. Dotted line outlines the northern valley of the Vema fracture zone

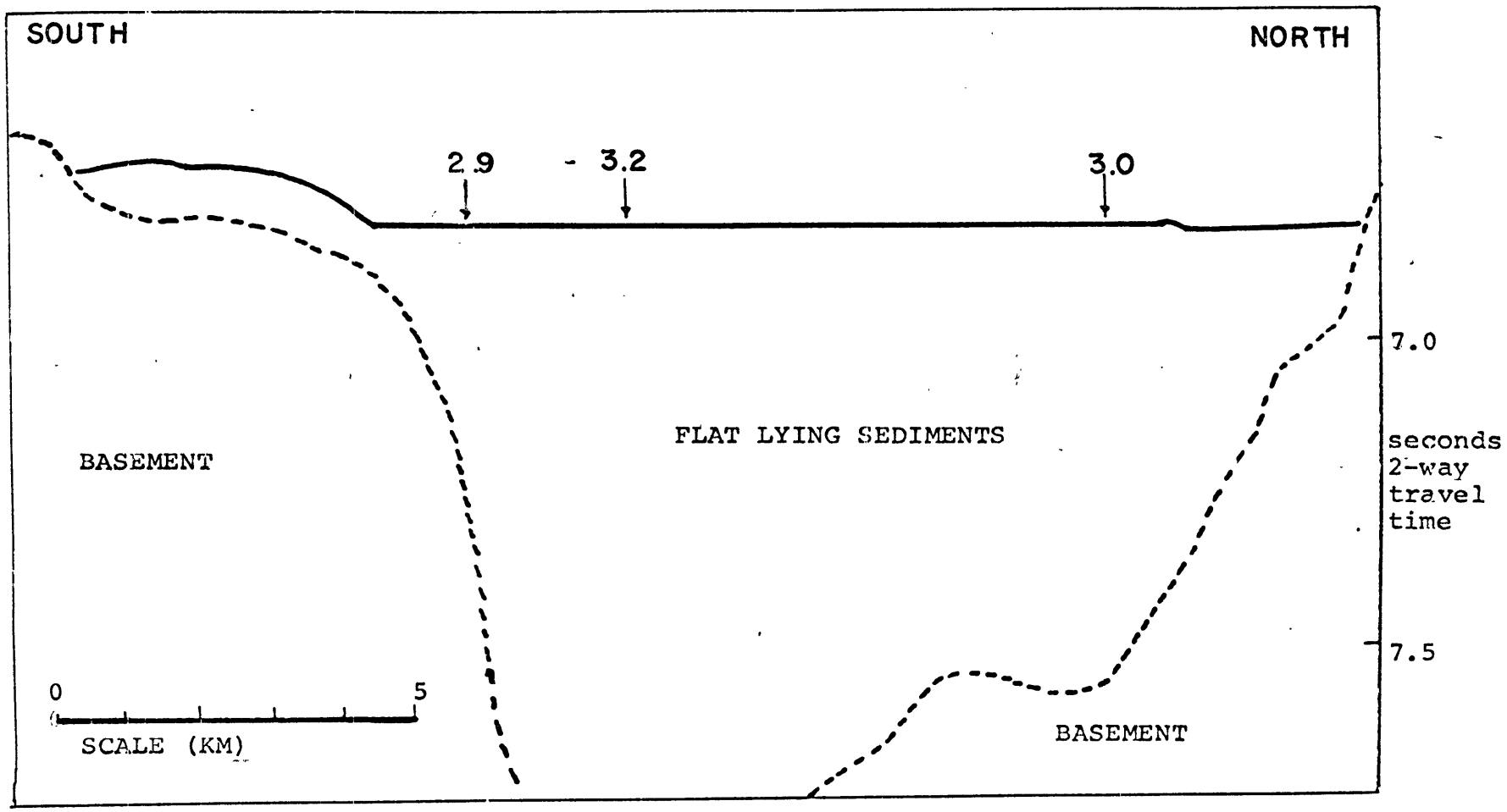

Fig. 7 3 heat flow measurements in a north-south profile across the northern valley of the Vema fracture zone. (structure from van Andel et al, 1967)

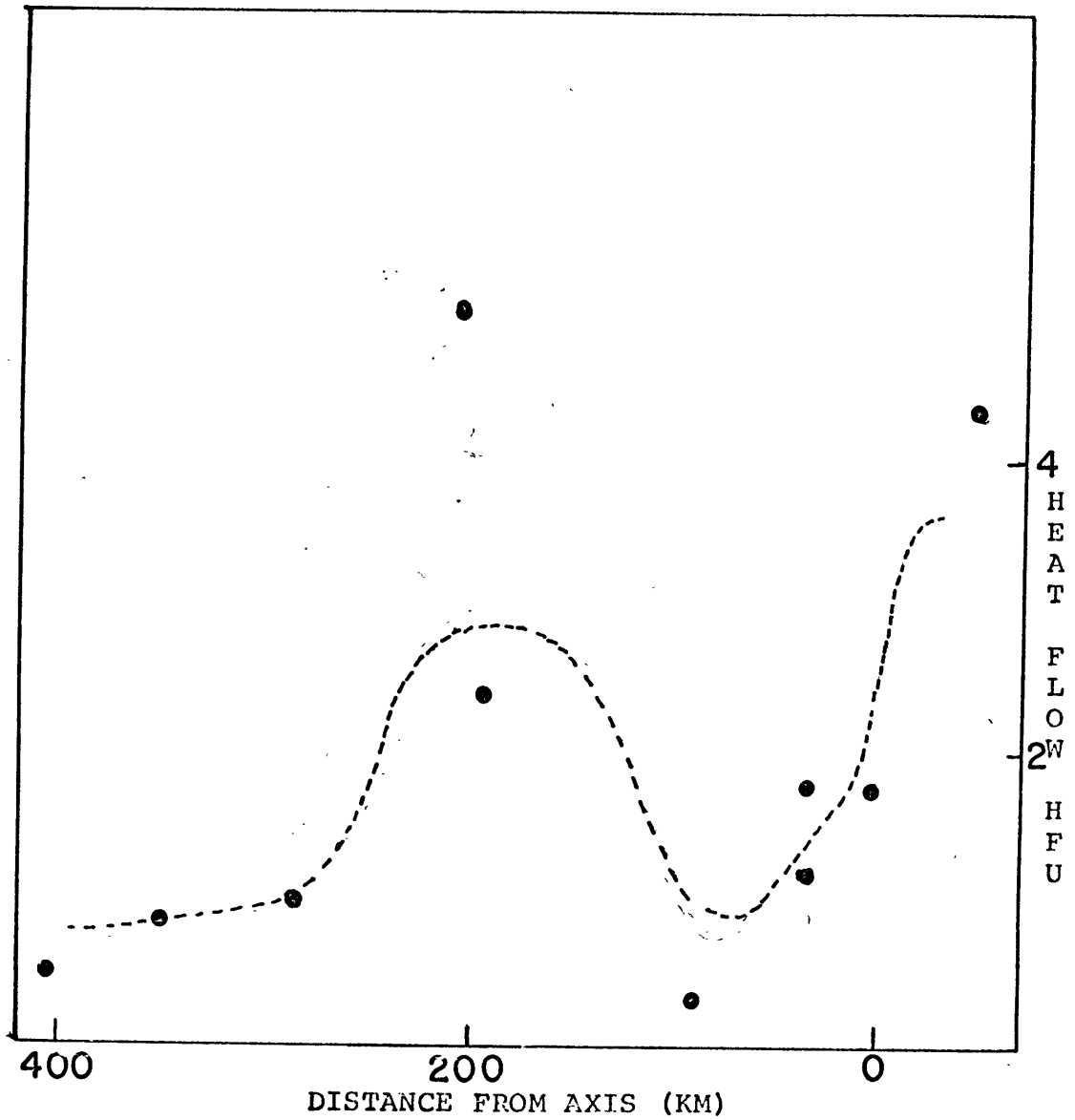

Fig. 8 Profile of heat flow in the Vema fracture zone excluding the measurements made in the northern valley

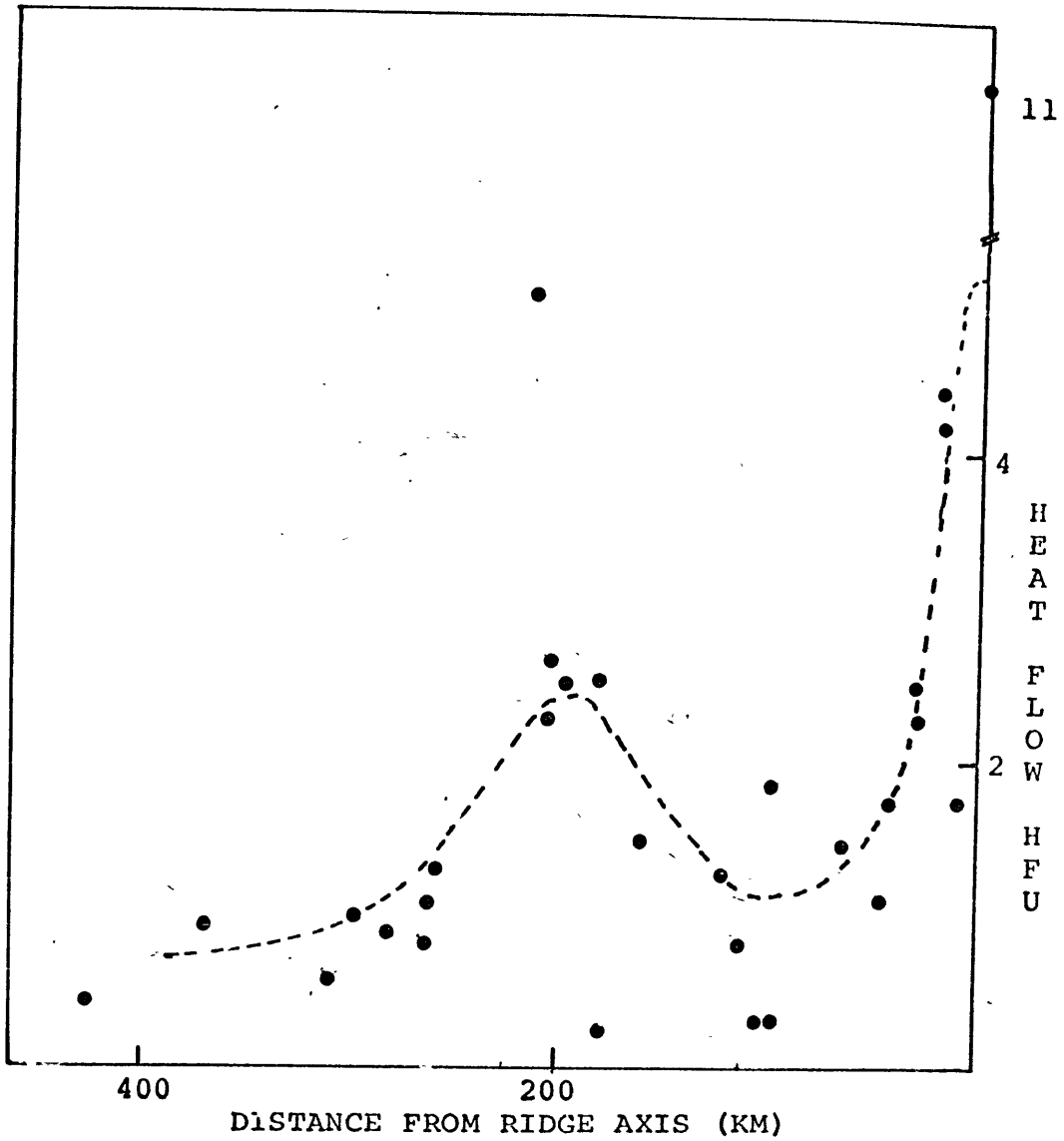

Fig. 9 Heat flow vs distance from the ridge axis for all heat flow measurements between 10°N and 14°N except those in the norther valley of the Vema fracture zone

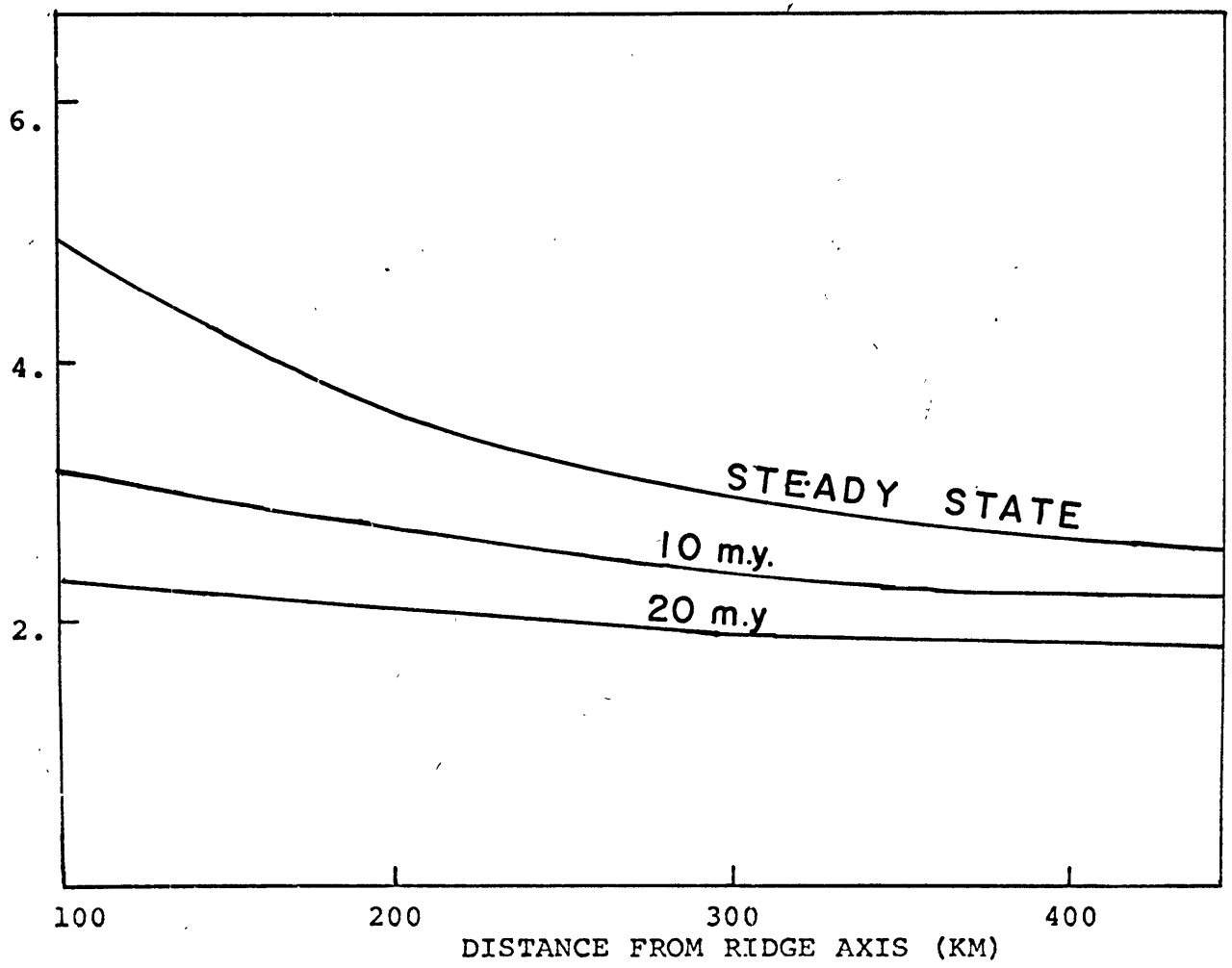

Fig. 10 The effect of differing periods of time (in millions of years) since sea floor spreading ceased on the heat flow (from Langseth et al, 1966)

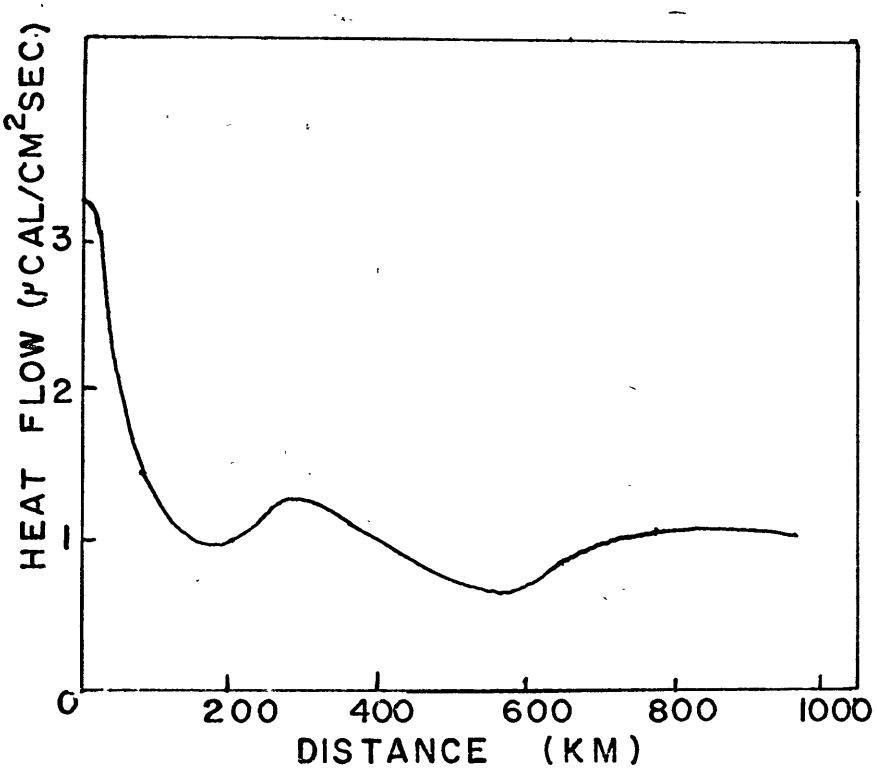

Fig. 11 Profile of heat flow vs. distance from the crest of the mid-Atlantic ridge. The 50 percentile line is plotted. (from Lee and Uyeda, 1965)

Table 1 Summary of heat flow data

Explanation of Table 1

STA - Station name

LAT - Latitude in degrees and minutes (North latitude except where indicated).

LON - Longitude in degrees and minutes West.

D - Corrected water depth in meters.

P - Penetration of corer in meters.

N - Number of sediment probes recording.

K - Thermal conductivity in mcal/cm sec ^{o}C.

GRAD- Gradient in ^{o}C/meter.

Q - These two columns contain the heat flow and the estimated error in heat flow in μ cal/cm^2sec. If no error limit is given it indicates the heat flow value is questionable.

Values for P and N were not available for the stations at which the short probe was used.

TABLE 1

STA	LAT	LON	D	P	N	GRAD	K	Q	
CH75-6	14 18	59 38	3366	3	2	.064	2.16	1.38	.1
CH75-7	14 14	58 24	3547	6	2	.033	2.17	0.72	.1
CH75-8	14 13	57 24	5180	6	3	.078	2.00	1.56	.1
CH75-11	14 18	52 33	5141	5	3	.067	2.13	1.43	.2
CH75-12	14 15	50 40	4780	8	3	.043	2.15	0.92	.1
CH75-14	14 19	48 06	4070	7	3	.012	2.42	0.29	?
CH75-15	13 54	47 02	4329	7	3	.053	2.25	1.19	.1
CH75-16	13 21	46 08	3717	6	3	.108	2.31	2.50	.2
CH75-17	13 16	42 51	4425	6	4	.013	2.30	0.30	.1
CH75-18	13 23	43 54	3660	9	4	.068	2.43	1.65	.1
CH75-19	13 25	44 40	3151	3	1	>.18	2.33	>4.2	
CH75-20	13 22	45 24	3565	9	4	.078	2.46	1.92	.1
CH75-29	12 58	44 32	3470	5	3	>.44	2.51	>11.	
CH75-30	12 57	44 46	3489	5	3	.103	2.25	2.32	.2
CH75-31	13 00	45 58	3224	7	5	.014	2.40	0.34	?
CH75-32	13 02	46 55	3072	4	2	.062	2.42	1.50	.2
CH75-35	13 04	49 35	4995	7	5	.035	2.30	0.81	.1
CH75-37	13 06	51 19	5016	7	5	.059	2.31	1.37	.1
CH75-39	12 15	54 15	4679	8	5	.060	2.23	1.34	.1
CH75-40	12 09	55 41	4531	5	3	.049	2.26	1.11	.2
CH75-42	12 11	57 55	2827	6	4	.053	2.27	1.20	.1
VFZ-1	00 02S	42 07	3841	5	4	.063	2.45	1.55	.1
VFZ-4	10 50	44 10	5336	5	3	.130	2.21	2.88	.2
VFZ-5	10 22	44 18	4950	4	2	.038	2.45	0.93	.2
VFZ-6	9 38	43 38	4630	6	3	.046	2.12	0.97	.2
VFZ-8	10 48	42 56	5180	4	3	.123	2.53	3.00	.3
VFZ-9	9 36	42 47	4370	5	3	.106	2.21	2.34	.2
VFZ-10	9 49	41 50	3733	6	4	.019	2.29	0.44	.1
VFZ-12	10 19	41 19	3180	5	3	.047	2.40	1.13	.3
VFZ-13	11 21	41 52	4200	5	3	.024	2.31	1.0	?
VFZ-14	11 32	42 43	3733	6	4	.052	2.55	1.32	.1
VFZ-16	11 57	46 10	4215	6	3	.028	2.36	0.66	.2
VFZ-17	11 54	48 25	4672	9	5	.068	2.34	1.59	.2
VFZ-19	18 03	59 07	5538	5	3	.057	2.35	1.34	.1
SP-1	10 36	44 52	4995			.021	2.25	0.47	.1
SP-2	10 55	44 08	5165			.130	2.27	2.95	.2
SP-3	10 51	44 08	5160			.143	2.24	3.22	.2
SP-5	11 06	42 52	3700			.021	2.40	0.53	.1
SP-6	10 22	42 51	4450			.227	2.23	5.06	.3
SP-7	10 00	40 34	3620			.168	2.57	4.31	.2
SP-8	11 06	41 17	3840			.043	2.40	1.03	.1
SP-9	11 21	42 02	3825			.100	2.30	2.30	.1
SP-11	11 54	45 16	3685			.061	2.30	1.40	.2
SP-12	11 58	47 04	4095			.177	2.32	4.10	.4
SP-14	21 28	60 32	5730			.060	2.30	1.38	.1
SP-15	24 33	61 42	5675			.076	2.31	1.76	.2

APPENDIX A

Explanation of the tables

The station name is at the top left of the page.

The position, water depth, water temperature in ^{o}C, and the number of the water probe are at the top right of the page.

In the table the column headings are:

D - the depth in cm below the sediment surface of the conductivity or temperature measurement

K - the conductivity in mcal/cm sec ^{o}C

K# - the number of the needle-probe used for the conductivity measurements (if the needle-probe number is given only for the top measurement, the same needle was used for all measurements at the that station)

TEMP - these 2 colums contain the temperature and the error in the temperature in ^{o}C

T# - the number of the sediment probe

GRADIENT- the gradient and error in the gradient in ^{o}C/meter between the two adjacent sediment probes

K.AV - the average conductivity and its error between the two adjacent sediment probes

Q - the heat flow and its error between the two adjacent sediment probes

At the bottom of the value of heat flow calculated for the station is given. The method of calculation is explained in the section on Instrumentation and Data Reduction.

Comments about the station are given below the table.

CHAIN 75- 6

POSITION 14 18'N, 59 38'W
DEPTH 3366 METERS
WATER TEMP 2.57
WATER PROBE# 287

D	K	K#	TEMP		T#	GRADIENT	K.AV	Q	
20	2.04	3							
45	2.00	2							
95	2.19	3							
140			2.698	.003	320				
145	2.20	2							
163	2.23	3							
207	2.11	2				.064	.004	2.21	1.41 .14
257	2.29	2							
307	2.25	3							
353			2.835	.006	363				

HEAT FLOW 1.38 .12

CHAIN 75- 7

POSITION 14 14'N, 58 24'W
DEPTH 3547 METERS
WATER TEMP 2.40
WATER PROBE# 287

D	K	K#	TEMP		T#	GRADIENT	K.AV	Q	
65	2.15	3							
115	2.17	2							
121			2.516	.003	296				
165	2.10	3							
215	2.13	2							
265	2.20	3				.033 .004	2.16	0.71	.13
315	2.26	2							
368	2.15	3							
384			2.570	.003	375				
418	2.28	2							
468	2.06	3							
510	2.21	2							
560	2.08	3							
610	2.31	2							

HEAT FLOW 0.72 .10

ABYSSAL HILLS 50 - 80 M HIGH

CHAIN 75- 8

POSITION 14 13'N, 57 24'W
DEPTH 5180 METERS
WATER TEMP 1.97
WATER PROBE# 287

D	K	K#	TEMP	T#	GRADIENT	K.AV	Q	
45	1.90	3						
70			2.129 .003	296				
95	1.98	2						
135	1.99	3						
195	1.98	2						
232			>2.287	375				
251	1.99	3			.078 .001	2.00	1.57	.08
301	2.09	2						
338	2.01	3						
388	2.04	2						
438	1.95	3						
442			2.421 .003	269				
495	2.02	2						
545	1.98	3						
595	2.05	2						

HEAT FLOW 1.56 .06

NEARLY FLAT, SLOPES SLIGHTLY TO THE WEST

CHAIN 75- 11

POSITION 14 18'N, 52 33'W
DEPTH 5141 METERS
WATER TEMP 1.82
WATER PROBE# 287

D	K	K#	TEMP	T#	GRADIENT	K.AV	Q	
72	2.28	2						
122	1.96	3						
172	1.99	2						
211			1.986 .003	296				
222	1.92	3						
242	2.27	3						
252	2.19	3						
272	2.50	2			.069 .003	2.12	1.46	.12
289	2.17	2						
326	1.99	3						
375	1.97	2						
408			2.122 .003	343				
426	2.04	3						
475	2.16	2						
525	2.11	3			.065 .005	2.11	1.38	.15
575	2.25	2						
588			2.239 .006	270				

HEAT FLOW 1.43 .16

SLIGHTLY UNDULATING NEAR WESTERN EDGE OF AN ABYSSAL PLAIN. WATER DEPTH INCREASES TO THE EAST

CHAIN 75- 12

POSITION 14 15'N, 50 40'W
DEPTH 4780 METERS
WATER TEMP 1.87
WATER PROBE# 269

D	K	K#	TEMP		T#	GRADIENT		K.AV	Q	
50	2.03	?								
210	2.03	2								
211			2.018	.005	296					
257	2.17	?								
307	2.19	2				.046	.005	2.15	0.99	.15
357	2.12	?								
415	2.22	?								
420			2.115	.005	320					
455	2.30	?								
507	2.22	2				.037	.006	2.25	0.83	.16
557	2.24	?								
589			2.178	.005	270					
610	2.15	3								
647	2.04	?								
707	2.03	3								
760	2.23	?								

HEAT FLOW 0.92 .09

ROUGH BOTTOM RELIEF, ABOUT 80 M

CHAIN 75- 14

POSITION 14 19'N, 48 6'W
DEPTH 4070 METERS
WATER TEMP 2.11
WATER PROBE# 269

D	K	K#	TEMP	T#	GRADIENT	K.AV	Q	
45	2.40	2						
63			2.166 .003	296				
90	2.35	2						
140	2.29	2			.028 .003	2.37	0.66	.09
190	2.38	2						
240	2.46	2						
269			2.224 .003	320				
290	2.41	2						
340	2.38	2			-.007 .003	2.42	-.16	.08
390	2.44	2						
439			2.207 .003	270				
440	2.49	2						
490	2.48	2						
540	2.49	2						
590	2.48	2						
640	2.46	2						

HEAT FLOW 0.29 ?

NOTE REVERSED GRADIENT BETWEEN 2ND AND 3RD PROBES
TOPOGRAPHY CONSISTS OF LARGE HILLS AND SEDIMENT PONDS
THE MEASUREMENT WAS MADE ON A HILL 4 KM WIDE AND
ABOUT 500 M HIGH

CHAIN 75- 15

POSITION 13 54'N, 47 2'W
DEPTH 4329 METERS
WATER TEMP 2.19
WATER PROBE# 269

D	K	K#	TEMP	T#	GRADIENT	K.AV	Q	
127	2.20	2						
179	2.08	3						
212			2.372 .005	296				
229	2.37	2						
264	2.19	3			.048 .005	2.28	1.09	.14
314	2.35	2						
364	2.21	3						
417			2.470 .005	320				
432	2.32	2						
482	2.24	3			.060 .007	2.24	1.34	.19
532	2.19	2						
572	2.21	3						
590			2.573 .008	270				
622	2.36	2						
672	2.21	3						
722	2.35	2						
772	2.10	3						
801	2.37	2						

HEAT FLOW 1.19 .13

SLIGHTLY UNDULATING HILLS ABOUT 40 M HIGH

CHAIN 75- 16

POSITION 13 21'N, 46 8'W
DEPTH 3717 METERS
WATER TEMP 2.51
WATER PROBE# 269

D	K	K#	TEMP		T#	GRADIENT	K.AV	Q	
12			2.528	.003	296				
36	2.48	3							
56	2.30	2							
112	2.37	3				.102	.004	2.40	2.45 .20
162	2.41	2							
212	2.42	3							
215			2.735	.005	320				
262	2.22	2							
298	2.23	3				.109	.005	2.26	2.46 .21
348	2.21	2							
390			2.926	.003	270				
						.111	.004	2.29	2.54 .20
610			3.170	.005	276				

HEAT FLOW 2.50 .15

HILLY, 100 - 200 M RELIEF

CHAIN 75- 17

POSITION 13 16'N, 42 51'W
DEPTH 4425 METERS
WATER TEMP 2.37
WATER PROBE# 269

D	K	K#	TEMP		T#	GRADIENT	K.AV	Q	
162			2.447	.003	296				
						.006 .002	2.31	0.14	.07
468			2.467	.003	320				
						.026 .004	2.31	0.60	.10
640			2.511	.003	270				
						.012 .003	2.31	0.28	.08
874			2.539	.003	276				
JAR1	2.31	3							
JAR2	2.02	2							

HEAT FLOW 0.30 .07

CORER PRETRIPPED. ONLY A SMALL AMOUNT OF SEDIMENT WAS RECOVERED ON THIS STATION.
NEARLY FLAT BOTTOM FOR 14 KM SOUTH OF THE STATION

CHAIN 75- 18

POSITION 13 23'N, 43 54'W
DEPTH 3660 METERS
WATER TEMP 2.51
WATER PROBE# 269

D	K	K#	TEMP	T#	GRADIENT	K.AV	Q	
40	2.41	2						
70	2.45	2						
120	2.39	2						
170	2.41	2						
212			2.658 .005	296				
220	2.40	2						
270	2.41	2			.068 .004	2.40	1.63	.16
320	2.40	2						
370	2.38	2						
418			2.799 .003	320				
420	2.35	2						
468	2.41	2						
470	2.39	2			.072 .004	2.42	1.74	.17
520	2.44	2						
570	2.53	2						
590			2.922 .003	270				
620	2.50	2						
670	2.47	2						
720	2.45	2			.063 .003	2.48	1.56	.13
820	2.51	2						
824			3.070 .003	276				

HEAT FLOW 1.65 .08

ON HILL NEAR EDGE OF 4 KM WIDE FLAT BASIN

CHAIN 75- 19

POSITION 13 25'N, 44 40'W
DEPTH 3151 METERS
WATER TEMP 2.71
WATER PROBE# 287

D	K	K#	TEMP	T#	GRADIENT	K.AV	Q
0			2.170 .003	296			
					>.18	2.33	>4.2
167			3.011 .003	320			
217	2.35	2					
265	2.35	3					
315	2.30	2					

HEAT FLOW 4.2

THE TOP PROBE DID NOT PENETRATE THE SEDIMENT. A LOWER LIMIT FOR THE HEAT FLOW IS OBTAINED BY ASSUMING THIS PROBE WAS IMMEDIATELY ABOVE THE SEDIMENT.
NEAR THE CREST OF THE MID ATLANTIC RIDGE IN A VALLEY

CHAIN 75- 20

POSITION 13 22'N, 45 24'W
DEPTH 3565 METERS
WATER TEMP 2.55
WATER PROBE# 269

D	K	K#	TEMP	T#	GRADIENT	K.AV	Q	
53	2.40	2						
103	2.37	3						
163	2.40	2						
213	2.63	3						
264			2.799 .003	296				
273	2.46	2						
323	2.40	3			.078 .004	2.45	1.91	.18
373	2.52	2						
423	2.43	3						
445			2.920 .005	287				
473	2.39	2						
523	2.42	3			.076 .005	2.43	1.85	.18
573	2.45	2						
623	2.43	3						
645			3.072 .003	285				
673	2.55	2						
733	2.47	3			.082 .004	2.49	2.04	.18
783	2.48	2						
833	2.51	3						
878			3.262 .005	276				

HEAT FLOW 1.92 .13

HILLY, 700 M RELIEF. HILLS APPEAR TO BE ABOUT 1.5 KM WIDE

CHAIN 75- 29

POSITION 12 58'N, 44 32'W
DEPTH 3470 METERS
WATER TEMP 2.70
WATER PROBE# 269

D	K	K#	TEMP		T#	GRADIENT	K.AV	Q
129	2.55	2						
186	2.61	2						
207			3.601	.007	296			
233	2.48	2						
292	2.44	2				>.43	2.51	>11.
342	2.61	2						
402	2.45	2	3.839		320			
445	2.54	2						
505	2.57	2						
552	2.49	2						
585			4.123		287			

HEAT FLOW >11.

THE LOWER TWO PROBES WERE OFF SCALE. ASSUMING THE CORER PENETRATED TO THE BASE OF THE WEIGHT STAND YIELDS A MINIMUM HEAT FLOW.

CHAIN 75- 30

POSITION 12 57'N, 44 46'W
DEPTH 3489 METERS
WATER TEMP 2.46
WATER PROBE# 269

D	K	K#	TEMP		T#	GRADIENT	K.AV	Q	
120	2.30	3							
160	2.32	2							
197			2.725	.006	296				
210	2.25	3							
260	2.30	2				.096	.006	2.25	2.16 .22
320	2.20	3							
370	2.24	2							
392			2.908	.006	320				
420	2.23	3							
470	2.21	2							
520	2.18	3				.109	.006	2.23	2.43 .22
570	2.31	2							
575			3.109		287				

HEAT FLOW 2.32 .16

SMALL HILLS, 40 - 100 M HIGH ABOUT 5 KM EAST OF MEDIAN VALLEY

CHAIN 75- 31

POSITION 13 0'N, 45 58'W
DEPTH 3224 METERS
WATER TEMP 2.64
WATER PROBE# 269

D	K	K#	TEMP	T#	GRADIENT	K.AV	Q	
149	2.30	3						
197			2.682 .006	296				
199	2.38	2						
249	2.33	3			.026 .008	2.37	0.62	.22
349	2.41	3						
393			2.732 .010	320				
399	2.42	2						
449	2.41	3			-.007 .009	2.41	-.17	.23
509	2.38	2						
554			2.721 .006	287				
559	2.44	3						
609	2.39	2			.036 .008	2.44	0.88	.23
659	2.48	3						
700			2.773 .006	285				
709	2.47	2						
759	2.35	3			.005 .007	2.41	0.12	.18
877			2.781 .006	276				

HEAT FLOW 0.34 .07

TOPOGRAPHY IS HILLY WITH 400 - 600 M RELIEF
THERE IS A REVERSED GRADIENT BETWEEN THE 2ND AND 3RD PROBES, AND A LOW GRADIENT BETWEEN THE 4TH AND 5TH PROBES. THIS MAY HAVE BEEN CAUSED BY A PERIODIC CHANGE IN THE BOTTOM WATER TEMPERATURE.

CHAIN 75- 32

POSITION 13 2'N, 46 55'W
DEPTH 3072 METERS
WATER TEMP 2.56
WATER PROBE# 269

D	K	K#	TEMP		T#	GRADIENT	K.AV	Q	
30	2.25	3							
72	2.46	3							
100			2.680	.005	276				
102	2.30	3							
152	2.34	3				.062 .006	2.42	1.50	.21
202	2.34	3							
272	2.71	3							
277			2.790	.005	285				
322	2.67	3							
372	2.46	3							

HEAT FLOW 1.50 .15

STATION ON TOP OF LARGE HILL. AFTER LEAVING THE STATION THE WATER DEPTH INCREASED 1400 M IN 1. KM

CHAIN 75- 35

POSITION 13 4'N, 49 35'W
DEPTH 4995 METERS
WATER TEMP 1.84
WATER PROBE# 302

D	K	K#	TEMP		T#	GRADIENT	K.AV	Q	
41	2.09	3							
111	2.16	3							
141	2.19	3							
240			1.962	.005	364				
						.063	.024	2.20	1.38 .58
381			2.051	.034	290				
						.028	.025	2.20	0.62 .53
538			2.095	.005	348				
						.033	.007	2.30	0.76 .19
698			2.148	.005	314				
						.026	.006	2.30	0.60 .17
862			2.190	.005	314				

HEAT FLOW 0.81 .09

CONDUCTIVITY MEASUREMENTS WERE AVAILIBLE ONLY FOR THE PILOT CORE.

CHAIN 75- 37

POSITION 13 6'N, 51 19'W
DEPTH 5016 METERS
WATER TEMP 1.72
WATER PROBE# 332

D	K	K#	TEMP		T#	GRADIENT	K.AV	Q	
240			1.864	.005	364				
337	2.38	3				.056	.007	2.36	1.32	.19
387	2.34	3							
391			1.949	.005	298				
430	2.23	3							
487	2.23	3				.064	.006	2.25	1.44	.18
537	2.29	3							
538			2.043	.005	348				
607	2.37	3				.066	.006	2.33	1.54	.19
657	2.27	3							
698			2.148	.005	347				
707	2.33	3				.047	.006	2.33	1.10	.18
862			2.225	.005	314				

HEAT FLOW 1.37 .09

SLIGHTLY UNDULATING HILLS 40 M RELIEF

CHAIN 75- 39

POSITION 12 15'N, 54 15'W
DEPTH 4679 METERS
WATER TEMP 1.99
WATER PROBE# 332

D	K	K#	TEMP	T#	GRADIENT	K.AV	Q	
105	2.03	3						
155	2.19	3						
205	2.01	3						
240			2.232 .003	364				
255	2.19	3						
315	2.20	3			.050 .004	2.19	1.10	.12
366	2.18	3						
391			2.308 .003	298				
416	2.20	3						
476	2.25	3			.068 .005	2.22	1.51	.16
526	2.20	3						
538			2.408 .005	348				
576	2.19	3						
626	2.24	3			.054 .006	2.23	1.20	.18
676	2.26	3						
698			2.495 .005	347				
726	2.28	3						
776	2.45	3			.059 .006	2.38	1.40	.19
826	2.41	3						
862			2.604 .005	314				
876	2.34	3						

HEAT FLOW 1.34 .09

NEARLY FLAT ABYSSAL PLAIN SLOPING SLIGHTLY TO THE WEST.

CHAIN 75- 40

POSITION 12 9'N, 55 41'W
DEPTH 4531 METERS
WATER TEMP 1.93
WATER PROBE# 332

D	K	K#	TEMP	T#	GRADIENT	K.AV	Q	
177	2.15	3						
240			2.165 .009	364				
242	2.26	3						
292	2.19	3			.073 .009	2.23	1.63	.26
342	2.24	3						
391			2.275 .005	298				
392	2.15	3						
442	2.15	3			.024 .007	2.15	0.52	.17
538			2.310 .005	348				
542	2.19	3						
592	2.20	3			.040	2.40	0.96	
692	2.24	3						
792	2.96	3						
862			2.440	314				

HEAT FLOW 1.11 .20

NEARLY FLAT ABYSSAL PLAIN,

CHAIN 75- 42

POSITION 12 11'N, 57 55'W
DEPTH 2827 METERS
WATER TEMP 2.58
WATER PROBE# 371

D	K	K#	TEMP	T#	GRADIENT	K.AV	Q	
215	2.21	3						
240			2.767 .012	327				
265	2.10	3						
315	2.18	3			.077 .016	2.16	1.66	.38
365	2.18	3						
392			2.884 .012	345				
415	2.20	3						
465	2.22	3			.069 .016	2.24	1.54	.40
515	2.29	3						
540			2.986 .012	357				
565	2.35	3						
625	2.35	3			.030 .016	2.33	0.70	.40
675	2.27	3						
698			3.033 .012	358				
725	2.37	3						
775	2.34	3			.046 .013	2.36	1.09	.35
825	2.32	3						
875	2.42	3						
873			3.115 .012	272				

HEAT FLOW 1.20 .10

VEZ - 1

POSITION 0 2'N, 42 7'W
DEPTH 3841 METERS
WATER TEMP 2.32
WATER PROBE# 287

D	K	K#	TEMP	T#	GRADIENT	K.AV	Q	
40	2.43	23						
50	2.46	23						
60			2.431 .003	305				
130	2.43				.059 .004	2.45	1.45	.14
229			2.529 .003	291				
230	2.46				.071 .004	2.46	1.74	.15
270	2.46							
397			2.649 .003	321				
					.054 .005	2.46	1.33	.17
564			2.740 .005	289				

HEAT FLOW 1.55 .09

UPPER CALIBRATION LINE LOST

VFZ - 4

POSITION 10 50'N, 40 10'W
DEPTH 5336 METERS
WATER TEMP 1.76
WATER PROBE# 287

D	K	K#	TEMP		T#	GRADIENT		K.AV	Q	
80	2.04	23								
114			1.993	.003	352					
180	2.21									
260	2.21									
330	2.21					.127	.003	2.20	2.80	.13
430	2.26									
450			2.421	.005	321					
530	2.36					.135	.006	2.36	3.18	.25
616			2.645	.005	299					

HEAT FLOW 2.88 .20

VEZ - 5

POSITION 10 22'N, 44 18'W
DEPTH 4950 METERS
WATER TEMP 1.87
WATER PROBE# 287

D	K	K#	TEMP		T#	GRADIENT	K.AV	Q	
80	2.35	23							
84			1.895	.007	352				
150	2.39								
200	2.59					.038	.008	2.49	0.94 .24
250	2.57								
256			1.960	.007	291				
260	2.78								
350	2.31								

HEAT FLOW 0.93 .22

VFZ - 6

POSITION 9 38'N, 43 38'W
DEPTH 4630 METERS
WATER TEMP 1.84
WATER PROBE# 253

D	K	K#	TEMP		T#	GRADIENT	K.AV	Q	
135	2.07	28							
215	2.24								
260			1.937	.005	261				
290	2.07					.067 .006	2.09	1.40	.20
380	2.10								
429			2.050	.005	277				
490	2.10								
590	2.16					.024 .009	2.14	0.51	.20
596			2.090	.010	304				

HEAT FLOW 0.97 .21

VFZ - 8

POSITION 10 48°N, 42 56°W
DEPTH 5180 METERS
WATER TEMP 1.75
WATER PROBE# 253

D	K	K#	TEMP	T#	GRADIENT	K.AV	Q	
10			1.755 .005	261				
80	2.46	28			.147 .006	2.30	3.38	.30
170	2.50							
179			2.000 .005	277				
270	2.52				.103 .006	2.55	2.63	.30
346			2.169 .005	304				
370	2.64							

HEAT FLOW 3.0 .3

THE DIFFERENCE BETWEEN THE WATER TEMPERATURE AND THE TEMPERATURE OF PROBE1 IS ONLY 0.005 DEG.C INDICATING THAT THIS PROBE IS LESS THAN 5 CM FROM THE SURFACE OF THE SEDIMENT. THE CONDUCTIVITY OF THE TOP PORTION OF THE SEDIMENT IS USUALLY 2.0 OR LESS. THE VALUE FOR K.AV HAS BEEN LOWERED TO TAKE THE EFFECT OF THIS LAYER INTO ACCOUNT. THIS REDUCES THE DIFFERENCE IN THE HEAT FLOW MEASURED BETWEEN THE TWO SETS OF PROBES.

VEZ - 9

POSITION 9 36'N, 42 47'W
DEPTH 4370 METERS
WATER TEMP 1.97
WATER PROBE# 287

D	K	K#	TEMP		T#	GRADIENT	K.AV	Q	
50	2.19	28							
83			2.162	.005	352				
150	2.16					.104 .007	2.20	2.29	.22
256			2.342	.010	291				
400	2.28					.107 .005	2.26	2.42	.19
586			2.695	.005	299				

HEAT FLOW 2.34 .16

VEZ - 10

POSITION 9 49'N, 51 50'W
DEPTH 3733 METERS
WATER TEMP 2.19
WATER PROBE# 287

D	K	K#	TEMP		T#	GRADIENT	K.AV	Q	
50	2.32	29							
84			2.345	.008	352				
150	2.29					.014 .005	2.30	0.32	.13
250	2.27								
257			2.384	.005	291				
						.010 .006	2.27	0.23	.14
420			2.401	.005	321				
						.028 .006	2.27	0.63	.14
587			2.447	.005	299				

HEAT FLOW 0.44 .10

VFZ - 12

POSITION 10 19'N, 41 19'W
DEPTH 3180 METERS
WATER TEMP 2.65
WATER PROBE# 253

D	K	K#	TEMP	T#	GRADIENT	K.AV	Q	
100	2.32	28						
210			2.872 .010	261				
250	2.47				.062 .010	2.38	1.48	.29
379			2.979 .007	277				
400	2.38							
500	2.45				.030 .010	2.42	0.73	.27
546			3.031 .010	304				

HEAT FLOW 1.13 .25

VFZ - 13

POSITION 11 21'N, 41 52'W
DEPTH 4200 METERS
WATER TEMP 2.34
WATER PROBE# 287

D	K	K#	TEMP	T#	GRADIENT	K.AV	Q	
86			2.326 .003	343				
100	2.21	28			.017 .003	2.24	0.38	.10
200	2.29							
254			2.355 .003	291				
300	2.40				.009 .003	2.35	0.21	.10
400	2.33							
425			2.370 .003	321				
					.050 .005	2.33	1.16	.11
586			2.455 .005	299				

HEAT FLOW 1.0 ?

THE REVERSED TEMPERATURE GRADIENT BETWEEN THE WATER PROBE AND THE FIRST SEDIMENT PROBE APPEARS TO BE DUE TO A REDUCTION IN THE BOTTOM WATER TEMPERATURE. THE HEAT FLOW CALCULATED FROM THE OVERALL GRADIENT IS LOW DUE TO THE REDUCTION IN THE BOTTOM WATER TEMPERATURE . THE REDUCTION WILL HAVE THE SMALLEST EFFECT ON THE GRADIENT BETWEEN THE BOTTOM TWO PROBES WHERE THE MEASURED HEAT FLOW IS 1.16 HFU.

VFZ - 14

POSITION 11 32'N, 42 43'W
DEPTH 3733 METERS
WATER TEMP 2.45
WATER PROBE# 287

D	K	K#	TEMP		T#	GRADIENT	K.AV	Q	
75	2.56	28							
84			2.531	.003	343				
225	2.44					.065 .003	2.48	1.60	.10
256			2.642	.003	291				
375	2.66					.041 .005	2.66	1.09	.16
425			2.711	.005	321				
						.054 .005	2.66	1.44	.17
587			2.799	.003	299				

HEAT FLOW 1.32 .12

VEZ - 16

POSITION 11 57'N, 46 10'W
DEPTH 4215 METERS
WATER TEMP 2.00
WATER PROBE# 287

D	K	K#	TEMP		T#	GRADIENT	K.AV	Q	
75	2.34	28							
150	2.33								
256			2.204	.005	291				
300	2.51					.015 .006	2.42	0.36	.16
425			2.229	.005	321				
450	2.26					.041 .006	2.26	0.93	.16
586			2.295	.005	299				

HEAT FLOW 0.66 .18

VEZ - 17

POSITION 11 54'N, 48 25'W
DEPTH 4672 METERS
WATER TEMP 1.86
WATER PROBE# 287

D	K	K#	TEMP		T#	GRADIENT	K.AV	Q	
75	2.20	28							
83			1.913	.015	343				
150	2.33					.062 .014	2.28	1.41	.30
250	2.29								
256			2.020	.010	291				
350	2.28					.053 .012	2.29	1.21	.28
425			2.110	.010	321				
450	2.36					.093 .012	2.37	2.20	.28
587			2.260	.010	299				
600	2.41					.064 .025	2.47	1.58	.60
750	2.52								
867			2.440	.060	289				

HEAT FLOW 1.59 .21

VEZ - 19

POSITION 18 3'N, 59 7'W
DEPTH 5538 METERS
WATER TEMP 1.96
WATER PROBE# 287

D	K	K#	TEMP	T#	GRADIENT	K.AV	Q	
75	2.11	28						
125			2.070 .004	321				
150	2.31				.058 .005	2.25	1.30	.14
250	2.18							
287			2.164 .004	299				
350	2.39							
450	2.46				.056 .003	2.44	1.25	.12
550	2.46							
567			2.320 .004	289				
650	2.56							

HEAT FLOW 1.34 .13